Contribution from the Istituto di Chimica Generale e Inorganica, University of Florence, Laboratorio CNR, Florence, Italy

ESR Spectra of Low-Symmetry High-Spin Cobalt(II) Complexes. 6.[1] 6-Methylquinoline, Pyridine, and Water Adducts of Cobalt(II) Acetylacetonate

A. BENCINI, C. BENELLI, D. GATTESCHI,* and C. ZANCHINI

Received December 18, 1979

The single-crystal ESR spectra of the base adducts of cobalt(II) acetylacetonate with 6-methylquinoline, pyridine, and water have been recorded. The g values are in each case anisotropic, the $g_\perp$ splitting increasing on passing from 6-methylquinoline to pyridine and water. For the last case also the cobalt hyperfine splitting was resolved, and evidence of large second-order and nuclear quadrupole effects was found. The spin Hamiltonian parameters are discussed within an angular overlap formalism.

Introduction

The base adducts of cobalt(II) acetylacetonate have been studied with several techniques.[2-7] In particular ^{1}H resonance spectra[8] showed the presence of sizable dipolar interactions originated by magnetic anisotropy such that $g_\perp > g_\parallel$. We have recently shown that the pattern of g values in the tetragonally distorted octahedral cobalt(II) complexes is dramatically affected by the π-bonding ability of the equatorial and axial ligands.[9] It appeared to us of interest to study the cobalt(II) acetylacetonate adducts with various ligands in order to determine how the principal g values and directions are affected by the nature of the axial substituents.

We wish to report here the ESR spectra of $Co(acac)_2L_2$ (L = 6-methylquinoline (6-Mequin), pyridine, water) and their interpretation using the angular overlap model we have been using for the analyses of several other high-spin cobalt(II) complexes.[10,11]

Experimental Section

The $Co(acac)_2(6\text{-Mequin})_2$ complex was prepared as previously reported,[12] and suitable single crystals were obtained by slow evaporation of solutions of methylene chloride. The crystals, monoclinic and elongated along b, were oriented by Weissenberg techniques.

The pyridine adduct was synthesized by adding stoichiometric amounts of the base to solutions of $Co(acac)_2(H_2O)_2$ in acetone. We were able to obtain monoclinic crystals[1,13] but were not able to obtain orthorhombic ones.[14]

The doped single crystals of $(Co,Mg)(acac)_2(H_2O)_2$ were obtained from dimethylformamide solutions of the two complexes with the Co/Mg ratio in the range 0.08–0.05. Also these monoclinic crystals,[15,16] elongated along b, were oriented by Weissenberg techniques, and the (100) face was the most developed.

Single-crystal ESR spectra down to 4.2 K were recorded with a Varian E-9 spectrometer operating at 9 GHz, equipped with an Oxford Instruments ESR 9 continuous-flow cryostat. The crystals were rotated by means of a Perspex rod and a goniometer. All the spectra were recorded at a microwave power of 1 mW.

All the calculations were performed with a SEL 32/77 computer from our laboratory.

Table I. Principal g Values and Directions for $Co(acac)_2(6\text{-Mequin})_2$

g	crystallographic frame[a]			molecular frame[b]		
5.665 (6)	0.7817	0.3959	0.4819	0.9997	−0.0048	−0.0161
4.11 (3)	0.6041	−0.2889	0.7427	0.0102	0.9348	0.3551
1.902 (4)	0.1548	−0.8717	0.4650	0.0134	−0.3552	0.9357

[a] The crystallographic frame is a^*bc. [b] The molecular frame is centered on the metal atom with z parallel to the metal-axial ligand direction and x parallel to a projection of the metal-oxygen bond direction in the plane orthogonal to z.

Results

The polycrystalline powder ESR spectra of $Co(acac)_2L_2$ (L = 6-methylquinoline (I), pyridine (II), and water (III)) are shown in Figures 1 and 2. No suitable diamagnetic host lattice was found for I and II, while for III both the pure and magnesium-doped complexes were studied. As previously observed[10,11] the large magnetic anisotropy of the cobalt(II) complexes is such that intermolecular exchange interactions do not determine exchange narrowing, and the signals of the individual molecules are resolved also in the pure compound. Only the hyperfine splitting is not resolved in these spectra. The close similarity of ESR spectra of the pure and the magnetically doped compounds shows that the structure of the cobalt complex remains substantially unchanged when it enters the magnesium lattice.

The single-crystal ESR spectra of I allowed us to obtain more precise values of the **g** tensor. The angular dependence of $\mathbf{g}^2$ in the three experimental rotations is given in Figure 3. The principal values and directions were obtained through a least-squares analysis, by using the Schonland method,[17] and are given in Table I. The smallest g value is found to be close to the cobalt axial bond direction. The angle of g_3 to this direction is $\sim 19°$; as a consequence the g_1 and g_2 directions do not lie exactly in the equatorial plane. The projection of g_1 and g_2 in the CoO_4 plane is practically parallel to the Co–O bond direction. The orientation of the **g** tensor in the molecular frame is shown in Figure 4.

Only the space group of II has been determined.[13] The single-crystal data yielded $g_1 = 5.833$, $g_2 = 3.919$, and $g_3 = 1.980$. A comparison of these data with magnetic susceptibility data is satisfactory. In particular, the maxima and minima of the g values in the ac plane are found to be within 5° from the corresponding extremes seen in the magnetic anisotropy experiment.[2]

The single-crystal ESR spectra of III are more complicated. In many orientations of the crystal in the static magnetic field, magnetic quadrupole effects are operative as shown by the presence of intense "forbidden" $\Delta M_I = \pm 1$ transitions. Some representative spectra are shown in Figure 5. The spacings between neighboring hyperfine lines are in general not equal,

(1) Part 5: Bencini, A.; Benelli, C.; Gatteschi, D.; Zanchini, C. *J. Mol. Struct.* **1980**, *60*, 401.
(2) Gerloch, M.; McMeeking, R. F.; White, A. M. *J. Chem. Soc., Dalton Trans.* **1976**, 655.
(3) Horrocks, W. DeW.; Hall, D. DeW. *Coord. Chem. Rev.* **1971**, *6*, 147.
(4) Cotton, F. A.; Elder, R. C. *Inorg. Chem.* **1966**, *5*, 423.
(5) Cotton, F. A.; Eiss, R. *J. Am. Chem. Soc.* **1968**, *90*, 38.
(6) Fackler, J. P., Jr. *Inorg. Chem.* **1963**, *2*, 266.
(7) Happe, J.; Ward, R. L. *J. Chem. Phys.* **1963**, *39*, 1211.
(8) Horrocks, W. DeW.; Hall, D. DeW. *Inorg. Chem.* **1971**, *10*, 2368.
(9) Bencini, A.; Benelli, C.; Gatteschi, D.; Zanchini, C. *Inorg. Chem.*, in press.
(10) Bencini, A.; Benelli, C.; Gatteschi, D.; Zanchini, C. *Inorg. Chem.* **1979**, *18*, 2137.
(11) Bencini, A.; Benelli, C.; Gatteschi, D.; Zanchini, C. *Inorg. Chem.* **1979**, *18*, 2526.
(12) Hursthouse, M. B.; Malik, K. M. A.; Davies, J. E.; Harding, J. H. *Acta Crystallogr. Sect. B* **1978**, *B34*, 1355.
(13) Hashagen, J. T.; Fackler, J. P., Jr. *J. Am. Chem. Soc.* **1965**, *87*, 2821.
(14) Elder, R. C. *Inorg. Chem.* **1968**, *7*, 1117.
(15) Bullen, G. J. *Acta Crystallogr.* **1959**, *12*, 703.
(16) Morosin, B. *Acta Crystallogr.* **1967**, *22*, 315.
(17) Schonland, D. S. *Proc. Phys. Soc., London* **1959**, *73*, 788.

0020-1669/80/1319-3027$01.00/0 © 1980 American Chemical Society

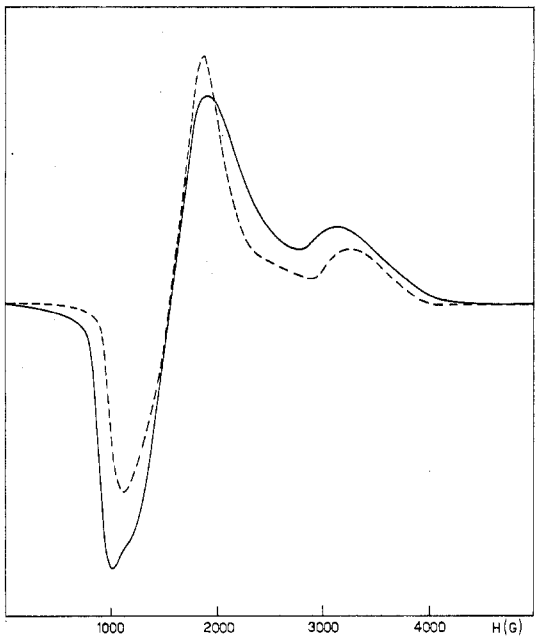

Figure 1. Polycrystalline powder ESR spectra of $Co(acac)_2(py)_2$ (—) and $Co(acac)_2(6\text{-Mequin})_2$ (---) recorded at X-band frequency at 4.2 K in the range 0–5000 G.

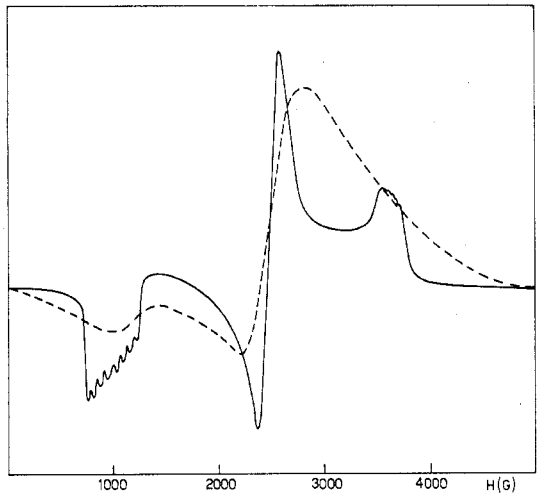

Figure 2. Polycrystalline powder ESR spectra of $(Co,Mg)(acac)_2(H_2O)_2$ (—) and $Co(acac)_2(H_2O)_2$ (---) recorded at X-band frequency at 4.2 K in the range 0–5000 G.

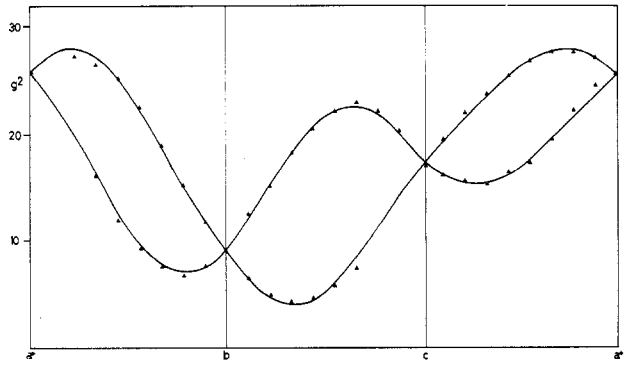

Figure 3. Angular dependence of the g^2 tensor of $Co(acac)_2(6\text{-Mequin})_2$ in the rotation about, from left to right, the *c*, *a**, or *b* crystal axis. The curves correspond to the least-squares fit to the experimental points.

showing that second-order corrections are operative. A first-order analysis of the data provided the principal *g* values

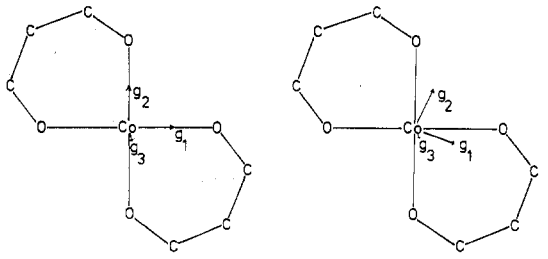

Figure 4. Principal directions of the **g** tensor projected in the plane orthogonal to cobalt–axial ligand bond direction for $Co(acac)_2(6\text{-Mequin})_2$ (left) and $Co(acac)_2(H_2O)_2$ (right).

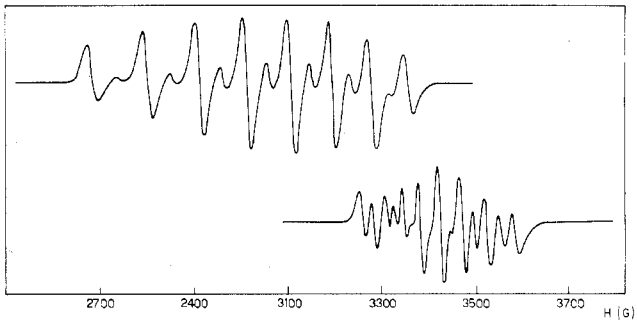

Figure 5. Single-crystal ESR spectra of $(Co,Mg)(acac)_2(H_2O)_2$ recorded at X-band frequency at 4.2 K. The static magnetic field is in the *bc* plane, making an angle of 30° from *b* (upper) and 40° from *b* (lower).

Table II. Principal *g* and *A* Values and Directions for $Co(acac)_2(H_2O)_2$

g	crystallographic frame[a]			molecular frame[a]		
6.84	0.3126	−0.7184	−0.6214	0.9040	−0.3822	−0.1896
2.74	0.9213	0.3885	0.0142	0.3983	0.9152	0.0535
1.88	−0.2312	0.5769	−0.7834	0.1531	−0.1239	0.9804
A[b]	crystallographic frame[a]			molecular frame[a]		
180	0.3384	−0.7066	−0.6214	0.9150	−0.3562	−0.1872
20	0.9066	0.4217	0.0142	0.3758	0.9227	0.0809
39	−0.2520	0.5682	−0.7834	0.1439	−0.1444	0.9790

[a] See the notes to Table I. [b] $cm^{-1} \times 10^{-4}$.

and directions, but the *A* values could not be determined in this way. With use of eq 35 reported by Rockenbauer and Simon[18] the transition fields were calculated for three experimental rotations. The transition fields were obtained by trial and error, in order to minimize the function $\sum_i (H_{io} - H_{ic})^2$ where H_{io} and H_{ic} are the observed and calculated transition fields for the orientation *i* in the static magnetic field. The fitting procedure was as follows: the *g* values and directions obtained by first-order analysis were used as starting parameters, together with *A* values estimated from the powder spectra. At this stage the *g* and *A* axes were not kept parallel to each other. The nine parameters (the principal values and the Euler angles relating the principal directions of *g* and *A* to the laboratory axes) were allowed to vary until the least-squares function was minimized. A last cycle was made by allowing *g* and *A* to be individuated by different Euler angles. However no substantial improvement to the fit was obtained. In Figure 6 are shown the experimental $\Delta M_I = 0$ transition fields in the three rotations, together with the calculated curves. The principal *g* and *A* values and directions are given in Table II. The **g** and **A** tensors are rotated by a small angle (~2°) which perhaps is not significant. If the principal directions are associated with one of the two magnetically nonequivalent

(18) Rockenbauer, A.; Simon, P. *Mol. Phys.* **1974**, *28*, 1113.

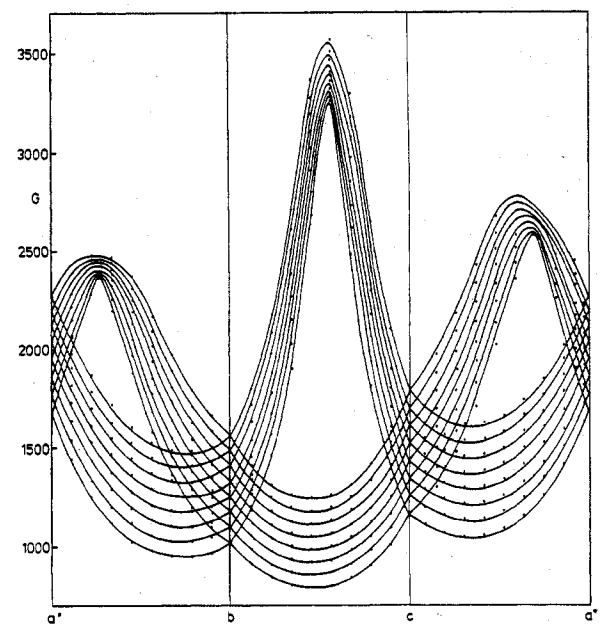

Figure 6. Angular dependence of observed transition fields $\Delta M_I = 0$, for $(Co,Mg)(acac)_2(H_2O)_2$ (●) in the rotation about, from left to right, the *c*, *a**, or *b* crystal axis. The curves are calculated with the method described in the text.

molecules in the cell,[19] it is found that g_3 makes an angle of $\sim 11°$ to the metal–water bond direction, while the projections of g_1 and g_2 on the cobalt–acetylacetonate plane make an angle of $\sim 22°$ to the Co–O bond direction. Figure 4 shows the orientation of the **g** tensor in the molecular frame. Since the intensities of the $\Delta M_I = \pm 1$ lines did not follow the simple pattern 21:16:5:0:5:16:21 or 7:12:15:16:15:12:7, which was expected for a dominant quadrupole or nuclear Zeeman interaction,[20] the required analysis appeared to be complicated, and it was not pursued further.

Discussion

The ESR data for the four complexes show completely anisotropic *g* values, with the rhombicity, $g_1 - g_2$, increasing drastically on passing from the nitrogen bases to the water adducts. The average of the g_1 and g_2 values, $g_\perp$, is only slightly varying in the series 4.89, 4.88, and 4.85 for I, II, and III, respectively, while g_3 decreases by 0.1 on passing from quinoline to water. Another relevant feature seen in the ESR spectra of these complexes is that the projections of the g_1 and g_2 axes in the CoO_4 molecular plane are practically parallel to the bond directions in I, while they are making angles of $\sim 20°$ in the case of III. No detailed X-ray information is available for II, so it will not be considered in the following. It is interesting to see if these variations can be justified on the basis of the structural parameters and of the bonding interactions in these complexes.

The structural characteristics of I and of the magnesium analogue of III are extremely similar,[13,16] as shown by the relevant data reported in Table III. The main difference between the two complexes, beyond the nature of the axial ligand, is given by the deviation of the metal atom from the acetylacetonate planes. The deviation can be simply described by the rotation, α, of the acetylacetonate planes around the O–O axis. The angle α is 16° for I and 20° for III.

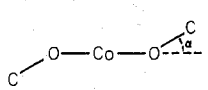

(19) Bencini, A.; Gatteschi, D. *Transition Met. Chem.*, in press.
(20) Chacko, V. P.; Manoharan, P. T. *J. Magn. Reson.* **1976**, *22*, 7.

Table III. Some Interatomic Distances (pm) and Bond Angles (Deg) in $Co(acac)_2(6\text{-Mequin})_2$[15] and $Mg(acac)_2(H_2O)_2$ Chromophores

	L = 6-Mequin	L = H_2O
	Interatomic Distances	
$M-O_1$	202.8	202.7
$M-O_2$	204.3	204.0
	Bond Angles	
O_1-M-O_2	89.3	89.0
O_1-M-L	89.5	88.5
O_2-M-L	91.9	90.9

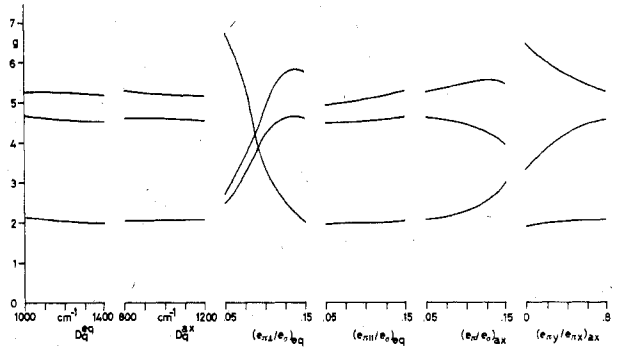

Figure 7. Dependence of calculated *g* values on bond parameters. From left the effect of varying: equatorial *Dq* (defined as $10Dq = 3e_\sigma - 2e_{\pi\perp}$) with $B = 800$ cm^{-1}, $\kappa = 0.85$, $\zeta = 533$ cm^{-1}, $Dq^{ax} = 900$ cm^{-1}, $(e_{\pi\perp}/e_\sigma)_{equat} = (e_{\pi\|}/e_\sigma)_{equat} = 0.15$, $(e_\pi/e_\sigma)_{axial} = 0.05$, and $(e_{\pi y}/e_{\pi x})_{axial} = 0.85$; axial *Dq* with the other parameters at the previous values and $Dq^{equat} = 1150$ cm^{-1}; the $e_{\pi\perp}/e_\sigma$ ratio for equatorial ligands; the $e_{\pi\|}/e_\sigma$ ratio for axial ligands; the $e_{\pi y}/e_{\pi x}$ ratio for axial ligands. The geometrical parameters were derived from the X-ray structure of $Co(acac)_2(6\text{-Mequin})_2$.

We have recently used the angular overlap model for the analysis of the ESR parameters of high-spin cobalt(II) complexes and were able to reproduce both the principal *g* and *A* values and directions by using parameters, e_λ,[21] which in principle depend on the nature of the metal–ligand bonding.[10,11] In the present case the e_σ^O, $e_{\pi\|}^O$, and $e_{\pi\perp}^O$ are required for the equatorial oxygen atoms ($\|$ and $\perp$ refer to the π interactions parallel and perpendicular to the tetragonal axis, respectively) and e_σ^L, $e_{\pi x}^L$, and $e_{\pi y}^L$ for the axial ligands. With the frame of reference we used, $e_{\pi x}$ gives the π interaction parallel to a projection of the cobalt–oxygen bond direction in the plane orthogonal to the metal–axial ligand direction. The 6-methylquinoline planes are approximately bisecting the angles outside the chelate rings.[12] Since it can be expected that the π interaction of quinoline with the metal atom is essentially orthogonal to the aromatic plane, in the chosen reference frame it can reasonably be assumed that $e_{\pi x}^N \simeq e_{\pi y}^N$. No such simplification is possible in the water complex since the positions of the hydrogen atoms are not available. The in-plane bond lengths are equal in the two complexes, so that the e_σ^O parameters can be assumed to be identical in both I and III. By neglect of the effect of the rotation by the angle α, the $e_{\pi\|}^O$ and $e_{\pi\perp}^O$ parameters can be considered to be identical in the two complexes.

A limitation on the value of the π parameters is given by expression 5 of ref 2 (eq 1). If Δ is negative, then $g_\| < g_\perp$

$$\Delta = 4e_{\pi\perp}^O - 2e_{\pi\|}^O - 2e_\pi^L \quad (1)$$

is observed.[9] Even with these simplifications the number of parameters is still high, so we tried to estimate the effect of their variations through sample calculations, which are shown

(21) Schäffer, C. E. *Pure Appl. Chem.* **1970**, *24*, 361.

Table IV. Best Fit of g Tensor and Its Principal Directions for $Co(acac)_2(6\text{-Mequin})_2$[a]

g values[b]				
obsd	calcd	calcd directions[c] in molecular frame		
5.67	5.69	0.9784	−0.1879	−0.0858
4.11	4.09	0.1842	0.9817	0.0489
1.90	2.05	0.0934	−0.0320	0.9951

[a] The diffuse reflectance electronic spectra at room temperature of the 6-methylquinoline adduct show envelopes of bands centered at 9.8, 19.9, and 27.7 × 10^3 cm^{-1}. Calculated transitions in the (5–25) × 10^3 cm^{-1} range consist of two groups centered at 9.8 and 20.4 × 10^3 cm^{-1}, respectively. [b] Parameters: $B = 800$ cm^{-1}; $\kappa = 0.81$; $\zeta = 533$ cm^{-1}; $e_\sigma{}^O = 4580$ cm^{-1}; $e_{\pi\perp}{}^O = 860$ cm^{-1}; $e_{\pi\parallel}{}^O = 515$ cm^{-1}; $e_\sigma{}^N = 3910$ cm^{-1}; $e_{\pi y}{}^N = 675$ cm^{-1}; $e_{\pi x}{}^N = 785$ cm^{-1}. [c] For the reference frame see note *b* in Table I.

diagramatically in Figure 7. The *Dq* values, defined in the caption to Figure 7, were used since they are familiar through the characterization of the electronic spectra of the octahedral complexes. The appropriate values of *Dq* for both the axial and the equatorial ligands were determined by comparison with the electronic spectra of I and III, which show bands at ~10 000 and 20 000 cm^{-1}. The electronic spectra show a red shift of the band at ~10 000 cm^{-1} on passing from pyridine to 6-methylquinoline and water, in accord with the spectrochemical series. As shown in Figure 7, the $e_\pi{}^L$ parameters of the axial ligand largely determine the anisotropy of the *g* values, in the sense that a larger $e_\pi{}^L/e_\sigma{}^L$ ratio increases the splitting of g_1 and g_2. This is qualitatively in line with the observation of a larger rhombicity of the *g* values of the water derivative as compared to the 6-methylquinoline one. As a matter of fact the e_π has in general been assumed to be small for pyridine-type ligands,[9,22] while the e_π/e_σ ratio of ~0.22 was estimated from the analysis of the electronic spectra of copper(II) Tutton salts.[23] Also the anisotropy of the interaction with the axial ligand determines a large splitting of g_1 and g_2.

Due to relation 1 there is a strong correlation among the e_π values of the axial and equatorial ligands. With use of small values of $e_\pi{}^L$ (L = 6-methylquinoline), comparable to those previously used,[2,9] fits can be found with $e_{\pi\parallel}{}^O > e_{\pi\perp}{}^O$, which seems to correspond to the current views on the nature of the interaction of the acetylacetonate with the metal ions.[2,24,25] However the principal *g* directions were not satisfactorily reproduced, since g_1 and g_2 are predicted to be rotated from the bond directions, contrary to the experimental findings. A better agreement with the experimental data is found by using larger $e_\pi{}^L/e_\sigma{}^L$ ratios, but in this case $e_{\pi\parallel}{}^O < e_{\pi\perp}{}^O$. The best fit we obtained is shown in Table IV.

Table V. Best Fit for g and A tensors and Their Principal Directions for $Co(acac)_2(H_2O)_2$[a]

g values[b]				
obsd	calcd	calcd directions in molecular frame[c]		
6.84	6.88	0.9954	−0.0826	0.0489
2.74	2.85	0.0876	0.9899	0.1112
1.88	1.93	0.0392	−0.1150	0.9926
A values[d]				
obsd	calcd	calcd directions in molecular frame[c]		
180	193	0.9965	−0.0751	−0.0370
20	23	0.0780	0.9936	0.0822
39	37	0.0306	−0.0848	0.9939

[a] The diffuse reflectance electronic spectra at room temperature of the H_2O derivative show envelopes of bands centered at 9.4, 20.0, 25.5, and 28.6 × 10^3 cm^{-1}. Calculated transitions in the (5–25) × 10^3 cm^{-1} range consist of two groups centered at 9.5 and 20.2 × 10^3 cm^{-1}, respectively. [b] Parameters: $B = 800$ cm^{-1}; $\kappa = 0.85$; $\zeta = 533$ cm^{-1}; $e_\sigma{}^O = 4500$ cm^{-1}; $e_{\pi\perp}{}^O = 795$ cm^{-1}; $e_{\pi\parallel}{}^O = 465$ cm^{-1}; $e_{\pi y}{}^{ax} = 550$ cm^{-1}; $e_{\pi x}{}^{ax} = 910$ cm^{-1}; $e_\sigma{}^{ax} = 3635$ cm^{-1}. [c] For the reference frame see not *b* in Table I. [d] cm^{-1} × 10^{-4}. AO parameters as for the *g* calculations. $P = 0.0160$ cm^{-1}; $\kappa = 0.30$.

A similar treatment for complex III requires a larger $e_\pi{}^L/e_\sigma{}^L$ ratio. The best fit is shown in Table V. The only way to obtain this fit was to consider the interaction of water largely anisotropic with $e_{\pi x}/e_{\pi y} = 1.67$.

In the present case also the hyperfine coupling tensor is available, and it was included in the calculation, by using the method previously described.[25] In the calculation two more parameters are involved, namely, $P = g_e g_n \mu_B \mu_n \langle r^{-3} \rangle_{av} = 0.0160$ cm^{-1} and κ, the isotropic Fermi interaction constant, = 0.30. The best results were obtained by using *P* and κ sensibly lower than the values calculated for the free ion[27,28] ($P = 0.0254$ cm^{-1}; $\kappa = 0.35$). It is, however, worth noting that the *A* values are reproduced quite well, in particular the somewhat unexpected feature of a quasi-axial **A** tensor, but with the unique "$A_\parallel$" value associated with one of the "$g_\perp$" components.

The present results show once more how the ESR spectra of low-symmetry high-spin cobalt(II) complexes can be understood by using the angular overlap model previously described.[10] In particular the variations seen in the *g* anisotropy and in the principal directions can be reproduced by allowing for the different $e_{\pi x}$ and $e_{\pi y}$ interactions of the axial ligands with the central metal ion. Although these fits are by no means unique, it is important for us that the data of I and III can be reproduced by using the minimum allowed number of parameters and varying their values according to the expectations on the nature of the ligand–metal interaction for 6-methylquinoline and water.

Registry No. I, 66712-49-0; II, 21361-39-7; III, 74111-86-7; $Mg(acac)_2(H_2O)_2$, 53447-39-5.

(22) Smith, D. W. *Inorg. Chem.* **1978**, *17*, 3153.
(23) Hitchman, M. A. *Inorg. Chem.* **1976**, *15*, 2150.
(24) Hitchman, M. A.; Belford, R. L. "Electron Spin Resonance of Metal Complexes"; T. F. Yen: London, 1969; p 97.
(25) Hitchman, M. A. *Inorg. Chem.* **1974**, *13*, 2218.
(26) Bencini, A.; Gatteschi, D. *J. Magn. Reson.* **1979**, *34*, 653.
(27) McGarvey, B. R. *Transition Met. Chem. (N.Y.)* **1966**, *3*, 89.
(28) McGarvey, B. R. *J. Phys. Chem.* **1967**, *71*, 51.